the past 150-year period of reported global warming.

Second, historical information on solar activity obtained from the C^{14} and Be^{10} records indicates that the present level of activity is about as high as any reached in the past several millennia (*13*). This reduces the likelihood that a future increase in solar activity beyond present levels might make the sun dimmer, decreasing its average output to levels that might fall below the 0.3% lower total irradiance estimated for the 17th-century Maunder Minimum (*7, 14*).

Finally, if transient magnetic activity levels much exceeding that of the sun at present are encountered in the future (or are shown to have occurred in the past), they are most likely to be associated with a dimming of the sun. This dimming should occur if the time scale of magnetic activity increase is short compared with the radiative relaxation time of layers storing the heat blocked by sunspots. This time scale could be as long as the radiative relaxation time of the solar convection zone, on the order of 10^5 years. Over longer time scales, one would expect the sun's luminosity to return to its average value, which is determined by nuclear burning rates and is unaffected by photospheric thermal impedances (*15, 16*). This suggests that a closer look at climate perturbations that may be associated with periods of anomalously high solar activity before the past few millennia might help to explain episodes of more pronounced climatic cooling than was produced by the Little Ice Age.

Higher (and lower) levels of solar irradiance may be achieved by other mechanisms than modulation by photospheric magnetism (*16*), and these could account for the correlations found between the Earth's temperature variations and several indices of solar activity (*17–19*). But further study of results from stellar photometry will be required to determine whether there exist sun-like stars exhibiting large luminosity variations that cannot be ascribed to photospheric magnetic activity. Discovery of such stars would be an important event for climate studies, because the imminent occurrence of such large solar luminosity variations would be much harder to rule out. Techniques for identifying such stars might include comparison of luminosity variation amplitudes measured on rotational time scales with those observed on much longer time scales. More detailed comparisons between the calcium-line variability and the photometric variability could also help in the discrimination.

REFERENCES AND NOTES

1. W. Lockwood, B. Skiff, S. Baliunas, R. Radick, *Nature* **360**, 653 (1992).
2. S. Baliunas and R. Jastrow, *ibid.* **348**, 520 (1990).
3. J. Hansen, A. Lacis, R. Ruedy, in *Climate Impact of Solar Variability*, K. Schatten and A. Arking, Eds. (NASA Conference Publication 3086, Washington, DC, 1990), pp. 135–145.
4. R. Willson and H. Hudson, *Nature* **332**, 810 (1988).
5. J. Hickey, B. Alton, H. Kyle, D. Hoyt, *Space Sci. Rev.* **48**, 321 (1988).
6. R. Lee *et al.*, *Metrologia* **28**, 265 (1991).
7. P. Foukal and J. Lean, *Astrophys. J.* **328**, 347 (1988).
8. P. Foukal, *Solar Phys.* **148**, 219 (1993).
9. J. Lawrence, *J. Geophys. Res.* **92**, 813 (1987).
10. C. Zwaan, in *The Sun as a Star*, S. Jordan, Ed. (NASA Publication SP-450, Washington, DC, 1981), pp. 163–180.
11. S. Saar, in *The Sun in Time*, C. P. Sonnett *et al.*, Eds. (Univ. of Arizona Press, Tucson, 1991), p. 848.
12. R. Radick, G. Lockwood, S. Baliunas, *Science* **247**, 39 (1990).
13. J. Jirikowic and P. Damon, *Clim. Change*, in press.
14. J. Lean, O. White, A. Skumanich, W. Livingston, *Eos* **73**, 244 (1992).
15. P. Foukal, L. Fowler, M. Livshits, *Astrophys. J.* **267**, 863 (1983); H. Spruit, *Astron. Astrophys.* **108**, 348 (1982).
16. H. Spruit, in *The Sun in Time*, C. P. Sonnett *et al.*, Eds. (Univ. of Arizona Press, Tucson, 1991), pp. 118–158.
17. G. Reid, *J. Geophys. Res.* **96**, 2835 (1991).
18. E. Friis-Christensen and K. Lassen, *Science* **254**, 698 (1991).
19. D. Hoyt, *Clim. Change* **2**, 79 (1979).

20. I am grateful to W. Lockwood, R. Radick, and S. Baliunas for discussion of their results. This work was supported by grant ATM-9222592 from the Solar-Terrestrial Program of NSF.

13 December 1993; accepted 15 February 1994

Trends in Stomatal Density and $^{13}C/^{12}C$ Ratios of *Pinus flexilis* Needles During Last Glacial-Interglacial Cycle

P. K. Van de Water, S. W. Leavitt, J. L. Betancourt*

Measurements of stomatal density and $\delta^{13}C$ of limber pine (*Pinus flexilis*) needles (leaves) preserved in pack rat middens from the Great Basin reveal shifts in plant physiology and leaf morphology during the last 30,000 years. Sites were selected so as to offset glacial to Holocene climatic differences and thus to isolate the effects of changing atmospheric CO_2 levels. Stomatal density decreased ~17 percent and $\delta^{13}C$ decreased ~1.5 per mil during deglaciation from 15,000 to 12,000 years ago, concomitant with a 30 percent increase in atmospheric CO_2. Water-use efficiency increased ~15 percent during deglaciation, if temperature and humidity were held constant and the proxy values for CO_2 and $\delta^{13}C$ of past atmospheres are accurate. The $\delta^{13}C$ variations may help constrain hypotheses about the redistribution of carbon between the atmosphere and biosphere during the last glacial-interglacial cycle.

Variations in atmospheric CO_2 affect the physiology and leaf morphology of C_3 plants, which dominate the terrestrial biosphere (*1*). These effects have been studied primarily in growth chamber experiments but also should be evident in fossil leaves from times in the past when CO_2 levels are known to have fluctuated. Evidence from ice cores indicates that ambient CO_2 levels varied from 190 to 200 parts per million by volume (ppmv) during glacial maxima to 270 to 280 ppmv during interglacials; relatively rapid increases have accompanied deglaciation (*2, 3*). The ice core evidence has inspired controlled experiments that simulate plant growth at glacial to present CO_2 concentrations (*4*). It also prescribes a reinterpretation of late Quaternary vegetation changes that acknowledges direct CO_2 effects, such as improved water use efficiency (WUE) at elevated CO_2 concentrations (*4*).

An abundance of leaves has been preserved in fossil pack rat middens from the western United States. These middens span the last 40,000 years with excellent coverage during deglaciation (*5*). We measured the stomatal density and $\delta^{13}C$ of fossil leaves of limber pine. During the last glacial period, this C_3 species dominated large expanses of open woodland in the lowlands of the Great Basin and the Colorado Plateau (*5*). Stomatal density and $\delta^{13}C$ are closely linked to carbon fixation and water status in C_3 plants and should be influenced by variations in CO_2 levels.

Stomatal densities decrease markedly as atmospheric CO_2 levels are increased from preindustrial (270 ppmv) to current values (350 ppmv), as seen in leaves from controlled experiments (*6, 7*) and herbarium specimens collected during the past 200 years (*7, 8*). Variations in stomatal densities have been used as a paleobarometer of atmospheric CO_2 variations during the last

P. K. Van de Water, Laboratory of Tree-Ring Research and Department of Geosciences, University of Arizona, Tucson, AZ 85721, USA.
S. W. Leavitt, Laboratory of Tree-Ring Research, University of Arizona, Tucson, AZ 85721, USA.
J. L. Betancourt, U.S. Geological Survey, Desert Laboratory, 1675 West Anklam Road, Tucson, AZ 85745, USA.

*To whom correspondence should be addressed.

10 million years (9), although ancient stomatal densities may be ineffective for inferring CO_2 levels above 350 ppmv (6).

Controls on the stable carbon isotopic composition of C_3 plants (*10*) are described by the equation (*11*)

$$\delta^{13}C_{plant} = \delta^{13}C_{air} - a - (b - a)\, C_i/C_a \quad (1)$$

where a and b are constants representing isotope fractionation by diffusion into the stomata (4.4 per mil) and by the enzyme ribulose-bisphosphate (RuBP) carboxylase (~27 per mil), respectively, and C_i and C_a are the concentrations of CO_2 in the intercellular leaf space and in the air, respectively. The value of $\delta^{13}C_{air}$ can change through anthropogenic processes or through alterations in the dynamics of ocean geochemistry and the terrestrial biosphere. If $\delta^{13}C_{air}$ remains constant, high values of C_i/C_a (more negative values of $\delta^{13}C_{plant}$) are promoted by high stomatal conductance, low rates of photosynthesis, and low WUE, and vice versa. Lower CO_2 levels during glacial times should have promoted increased stomatal densities and more negative $\delta^{13}C$ values in C_3 plants (through decreased WUE), unless $\delta^{13}C_{air}$ varied over time.

We measured stomatal densities (*12*) (Fig. 1) and $\delta^{13}C$ (*13*) (Fig. 2) of almost 1200 limber pine needles from 41 pack rat middens at elevations from 1320 to 2350 m in Idaho, Nevada, Utah, and Arizona (Table 1). Middens were dated to ^{14}C years, which we calibrated to calendar ages using tree rings (*14*) and mass spectrometric U-Th ages from Barbados corals (*15*). A potential source of error is the mixing of materials of different ages in the same midden, so that limber pine needles are not contemporaneous with the associated midden age. Using accelerator mass spectrometric (AMS) assays of ^{14}C, we tested two samples (Table 1) of the same CO_2 that was combusted from holocellulose for $\delta^{13}C$ analysis; in both cases, the AMS dates overlapped with the associated midden age at two standard deviations (~1320 and 1600 years). Also, we cannot determine if needles in a given sample came from a single tree, several trees, or several generations, nor can we eliminate the possibility of natural selection for either low or high CO_2 tolerance. Finally, correction of $\delta^{13}C_{plant}$ for elevation or latitudinal effects could impact calculations of key physiological parameters, such as C_i, $C_a - C_i$, and WUE (*13*).

The effects of climate change on temperature and humidity (vapor pressure gradient), and thus, on stomatal density and $\delta^{13}C$ values, were minimized by site selection. Because limber pine no longer occurs at our glacial sites, we developed the Holocene part of our chronology at higher elevations or more northerly latitudes. We selected sites in southern Idaho, near the lower limits of limber pine, that contain modern vegetation that closely resembles our glacial midden floras in southern Nevada, northern Arizona, and southern Utah. This approach is commonly used to reconstruct paleoclimates; the modern climate at the analog site approximates the paleoclimate at the glacial sites. Therefore, effective moisture and average annual temperatures were constant over the entire chronology, allowing focus

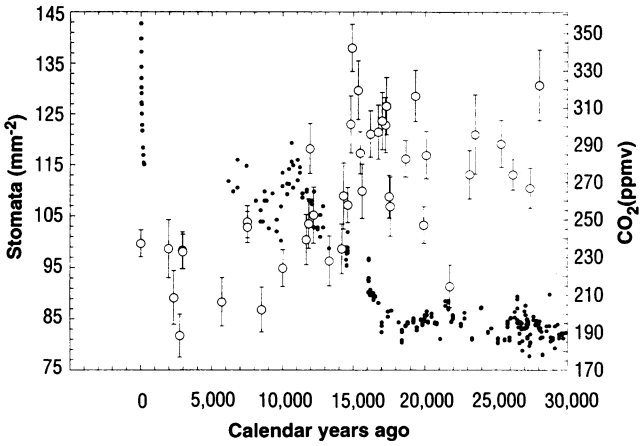

Fig. 1. Stomatal densities (open circles) in limber pine (*Pinus flexilis*) needles from fossil pack rat middens and CO_2 concentrations (solid circles) from the Byrd ice core for 30,000 to 6,000 years ago (*2, 3*), from the Siple Station ice core for 200 to 35 years ago (*27*), and from the Mauna Loa monitoring station for the last 35 years (*28*). Each point represents the mean and standard error of stomatal densities, with a range of 22 to 33 needles measured per data point. The modern sample consisted of needles pooled from 10 trees at Craters of the Moon National Monument in southern Idaho, in the general area of most of our Holocene samples.

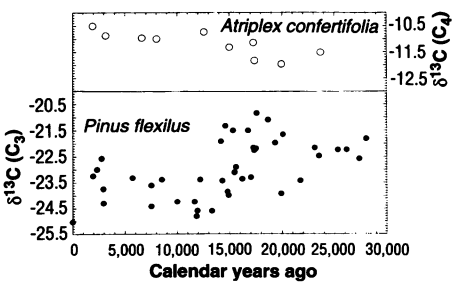

Fig. 2. The $\delta^{13}C$ of leaf cellulose from *Pinus flexilis*, a C_3 tree (this report), and *Atriplex confertifolia*, a C_4 halophytic shrub (*17*). The $\delta^{13}C$ of *Atriplex* presumably mirrors changes in $\delta^{13}C_{air}$, whereas the decreasing $\delta^{13}C$ of *Pinus flexilis* may be partly a response to increasing atmospheric CO_2. For *Pinus flexilis*, the modern sample is the same as in Fig. 1. On the basis of similar $\delta^{13}C$ values of ancient wood of equivalent age but varied percentages of undecomposed cellulose, Yapp and Epstein (*29*) found no evidence of decomposition-related isotope fractionation. Furthermore, fractionation through microbial degradation would tend to make older material lighter (more negative $\delta^{13}C$), which is the opposite of what we found.

Table 1. Stomatal densities and $\delta^{13}C$ values of limber pine leaves from fossil pack rat middens in the Great Basin.

Lat. (°N)	Long. (°W)	Elev. (m)	Age* (years ago)	Density (mm^{-2})	$\delta^{13}C$† (per mil)
43.28	113.55	1800	0	99.7	−25.0
43.93	113.43	1980	1960	98.6	−23.2
44.27	113.75	2180	2340	89.2	−23.0
43.65	113.13	1930	2760	81.8	−22.6
43.95	113.43	2230	2940	98.4	−23.7
43.95	113.43	2230	2960	98.1	−24.3
43.95	113.43	2230	5720	88.3	−23.3
39.50	114.72	2350	7510	103.9	−24.4
44.27	113.75	2180	7510	102.8	−23.6
43.95	113.43	2230	8420	86.9	−23.4
44.27	113.75	2180	10010	94.9	−24.2
37.80	109.60	2200	11660	100.4	−24.2
37.80	109.60	2200	11850	103.5	−24.8
37.80	109.60	2200	11930	118.2	−24.6
37.43	109.65	1590	12190	105.2	−23.4
37.80	109.60	2200	13300	96.3	−24.6
37.32	109.58	1390	14170	98.7	−21.9
36.25	111.95	2050	14300	109.0	−23.4
38.73	109.50	1320	14600	107.2	−21.3
37.32	109.58	1390	14810	123.0	−23.8
37.32	109.58	1390	14910	138.0	−24.0
37.40	109.63	1450	15340	129.7	−21.5
37.12	116.07	1810	15480	117.4	−23.1
37.98	109.72	1830	15620	109.9	−22.9
37.43	109.65	1585	16210	121.1	−23.4
37.12	116.07	1810	16750	121.5	−21.5
37.12	116.07	1810	17030	123.7	−23.3
37.12	116.07	1810	17250	122.9	−22.2
37.12	116.07	1810	17330	126.6	−22.3
38.73	109.50	1320	17506	108.8	−22.2
38.12	109.73	1510	17580	106.9	−20.8
37.12	116.07	1810	18650	116.3	−21.1
38.73	109.50	1320	19320	128.6	−22.0
36.17	111.92	1770	19900‡	103.3	−23.9
37.12	116.07	1810	20070	117.0	−21.7
36.17	111.92	1770	21740‡	91.4	−23.4
37.40	109.63	1450	23110	113.1	−22.2
38.73	109.50	1317	23510	121.0	−22.5
37.98	109.72	1830	25330	119.2	−22.2
37.00	109.73	1755	26170	113.2	−22.2
36.17	111.92	1770	27370	110.5	−22.6
37.98	109.72	1830	28020	130.7	−21.8

*The ^{14}C dates up to 7750 ± 120 years ago were converted to calendar years with the use of tree-ring calibrations (*14*). Older dates were corrected on the basis of U/Th ages of Barbados corals (*15*). †Normalized to modern sea level with 1.2 mil^{-1} km^{-1}. ‡AMS dates on same CO_2 combusted from holocellulose that yielded $\delta^{13}C$ values.

on the effects of changing CO_2 levels. Holocene sites (42.31°N, 2151 m) average ~5° farther north and ~400 m higher than our glacial sites (37.43°N, 1761 m). For a typical annual temperature decrease with latitude (−0.75°C per degree) and elevation (−6.5°C per kilometer), the difference between annual temperatures at our glacial and Holocene sites is ~6.4°C. Studies of elevational displacement of indicator species like limber pine in the Great Basin have implied that during glacial times, average annual temperatures were ~6° to 8°C colder than they are today, assuming no CO_2 effects on former plant distributions (5).

Stomatal density and $\delta^{13}C$ values both declined abruptly between 15 to 12 ka (thousand years ago) (Figs. 1 and 2). For comparison, we divided the last 30,000 years into three periods on the basis of the ice core record of atmospheric CO_2 levels: glacial (30 to 15 ka), transition (15 to 12 ka), and Holocene (since 12 ka). Average stomatal densities decreased 17% coincident with a 30% increase in atmospheric CO_2 from the glacial period to the Holocene (Table 2). Because stomatal densities are a function of the number of stomatal rows in an area for a given length and needle width, we also compared these attributes among the different periods. Needle width increased and the number of stomatal rows decreased from glacial to Holocene times (Table 2). The decrease in stomatal rows shows that lower stomatal densities are not a simple artifact of larger leaves (12).

Average Holocene $\delta^{13}C$ values were ~1.5 per mil more negative than glacial and ~0.6 per mil more negative than transition values. The abrupt decline in both stomatal density and $\delta^{13}C$ values occurred entirely during the transition. Despite similarities in the glacial to Holocene trends (Figs. 1 and 2), stomatal density is significantly correlated with $\delta^{13}C$ only during the Holocene ($R = -0.78$). This linkage could entail increased stomatal conductance with increased stomatal density (at constant CO_2 level). The lack of correlation during the glacial and transition periods may reflect variability introduced by greater site (and population) differences or to the greater instability of glacial and transition climates compared to that in the Holocene. Alternatively, stomatal density and isotopic discrimination may decouple in low CO_2 environments.

Limber pine $\delta^{13}C$ values of each period represent integrated measures of several physiological parameters (Table 3), which can be estimated by means of Eq. 1 and an equation for instantaneous WUE (16)

$$A/E\ (\mathrm{WUE}) = (C_a - C_i)/(1.6\nu) \quad (2)$$

where A is assimilation, E is transpiration, and ν is the gradient in water vapor pressure divided by total atmospheric pressure. We assumed that the average $\delta^{13}C_{air}$ values inferred from ice cores and C_4 plant cellulose (13, 17), as well as the C_a chronology derived from ice cores (13), are accurate. Plant discrimination (Δ) against ^{13}C of the atmosphere increases 12% from glacial (17.3 per mil) to Holocene (19.3 per mil) times. The C_i/C_a ratio increased 16.4% from glacial (0.55) to Holocene (0.64) times, but $C_a - C_i$ also increased 13.6% during this time (from 88.7 to 100.8 ppmv). In response to changing CO_2 concentrations, plant physiological strategy may be to keep either C_i/C_a or $C_a - C_i$ constant (18). Limber pine seems to have been unable to regulate either constant C_i/C_a or $C_a - C_i$ during deglaciation. The WUE increased 14.6% from glacial to Holocene times, if we assume that ν did not differ significantly between our glacial sites and their Holocene analogs; we cannot verify this assumption. However, such an increase in WUE is predicted from increased CO_2 concentration (19).

The lower glacial C_i/C_a ratios suggest that either stomatal conductance was lower or assimilation was greater than during the Holocene. The higher stomatal densities during the glacial period would seem to preclude lower stomatal conductance, but the theoretical linkage between stomatal density and stomatal conductance is uncertain (20, 21). The lower C_a in glacial times would suggest a 50% decrease in carbon assimilation (19), which could be offset by greater stomatal densities. Increased stomatal densities, measured as a significant reduction of leaf width as well as additional stomatal rows (Table 2), should reduce the pathway of diffusion for CO_2 into the leaf interior. Despite this, discrimination against ^{13}C at the site of carboxylation was reduced as CO_2 became less abundant, as reflected in elevated glacial $\delta^{13}C_{plant}$.

The limber pine $\delta^{13}C$ chronology may provide clues to shifts in the global carbon cycle over the last 30,000 years. If the glacial atmosphere was depleted in both CO_2 and ^{13}C (as suggested from ice cores and C_4 plants), then there must have been a corresponding larger size and ^{13}C enrichment of a terrestrial or ocean carbon reservoir. Although we recognize the importance of the ocean in controlling C_a and $\delta^{13}C_{air}$, the role of the terrestrial biosphere perhaps is not trivial. As a hypothetical exercise, we calculated mass balance assuming simple carbon exchange between the atmosphere and terrestrial biosphere and that our limber pine chronology is representative of $\delta^{13}C$ values for other C_3 plants

$$M_{Hb}(\delta_{Hb}) + M_{Ha}(\delta_{Ha}) = M_{Gb}(\delta_{Gb}) + M_{Ga}(\delta_{Ga}) \quad (3)$$

where masses of the Holocene terrestrial biosphere (M_{Hb}) and atmosphere (M_{Ha}) are 1.667×10^{17} and 6.233×10^{16} mol of C, respectively (22). The masses of glacial terrestrial biosphere (M_{Gb}) and atmosphere (M_{Ga}) are 1.860×10^{17} and 4.308×10^{16} mol, respectively, obtained by shifting 86 ppmv of CO_2 (172 gigatons of C) from the Holocene atmosphere (278 ppmv) to the glacial

Table 2. Chi-square contingency table for testing significance of differences between glacial (30 to 15 ka) (G), transition (15 to 12 ka) (T), and Holocene (12 to 0 ka) (H) measurements of stomatal frequency (in stomata per square millimeter), needle width (in millimeters), number of stomatal rows, and $\delta^{13}C$ (in per mil) in *Pinus flexilis* needles from fossil pack rat middens. For $\delta^{13}C$, we pooled needles for analysis, so that only 42 cases could be analyzed. The low case numbers violate one of the tenets of contingency table analysis; nevertheless, they should not significantly affect the differences between glacial and Holocene $\delta^{13}C$.

Period	Mean ± SE (N)	Chi-square analysis
	Stomatal density	
G	117.0 ± 1.0 (618)	G vs H 90.84***
T	111.1 ± 2.0 (200)	G vs T 5.37*
H	97.2 ± 1.6 (367)	H vs T 17.54***
	Needle width	
G	46.5 ± 0.2 (618)	G vs H 14.67***
T	44.9 ± 0.4 (200)	G vs T 6.78**
H	48.9 ± 0.3 (367)	H vs T 27.48***
	Stomatal rows	
G	2.06 ± 0.02 (381)	G vs H 26.85***
T	1.87 ± 0.04 (121)	G vs T 13.29***
H	1.87 ± 0.03 (211)	H vs T 0.35
	$\delta^{13}C$	
G	−22.31 ± 0.17 (21)	G vs H 14.08***
T	−23.21 ± 0.44 (7)	G vs T 5.19*
H	−23.80 ± 0.19 (13)	H vs T 0.43

*$P < 0.05$. **$P < 0.01$. ***$P < 0.001$.

Table 3. Summary of values used to calculate discrimination (Δ), C_i/C_a, $C_a - C_i$, C_i, and WUE for the glacial, transition, and Holocene periods.

Period	$\delta^{13}C_{air}$* (per mil)	$\delta^{13}C$† (per mil)	C_a‡ (ppmv)	Δ (per mil)	C_i/C_a	$C_a - C_i$ (ppmv)	C_i (ppmv)	WUE
Glacial	−6.92	−23.7	198.4	17.3	0.55	88.7	109.7	$55/\nu$
Transition	−6.62	−24.7	242.6	18.5	0.61	95.7	146.9	$60/\nu$
Holocene	−6.48	−25.3	278.5	19.3	0.64	100.8	177.7	$63/\nu$

*Average from (3, 17). †Limber pine whole-tissue values obtained by subtracting 1.5 per mil from holocellulose values (30). ‡Ice core C_a (3).

atmosphere (192 ppmv). The $\delta^{13}C$ of the Holocene (δ_{Hb}) and glacial (δ_{Gb}) terrestrial biospheres are −25.3 and −23.8 per mil from the limber pine results (averages in Table 2 have been adjusted by −1.5 per mil). Atmospheric $\delta^{13}C$ is −6.48 and −6.92 per mil for the Holocene (δ_{Ha}) and glacial (δ_{Ga}), respectively, from the ice core and C_4 data. Although perhaps coincidental, the mass balance of Eq. 3 is within 2% with these values. There is other evidence for a glacial, globally ^{13}C-enriched biosphere from terrestrial plants (*23*) and from marine sediment and organic $\delta^{13}C$ records (*24*). Low C_a values seem inconsistent with a large biosphere, but valid carbon cycle models must still account for the significant shifts in $\delta^{13}C$ of C_3 plants during the past 30,000 years.

We realize that stomatal density and $\delta^{13}C$ responses could vary widely, even among C_3 species. This variability could complicate their use in modeling the carbon and hydrological cycles. For example, average $\delta^{13}C$ values of gymnosperms may be ~1 per mil more positive than those of angiosperms (*25*); in theory, an increase in conifer relative to flowering plant biomass could sequester more ^{13}C from the atmosphere. Similarly, the sensitivity of stomatal density to changing CO_2 levels is less for gymnosperms than for angiosperms (*1*). As CO_2 increased from glacial to Holocene times, stomatal densities in limber pine decreased 17%, whereas in willow, they decreased by ~30% (*9*). Since industrialization, stomatal densities have dropped 20 to 40% in various angiosperms (*7–9*) but have not varied in limber pine (Fig. 2). Thus, stomatal densities in conifers may be sensitive to the lower CO_2 of glacial atmospheres but not to future CO_2 enrichment.

REFERENCES AND NOTES

1. F. I. Woodward, *Vegetatio* **104/105**, 145 (1993); _____, G. B. Thompson, I. F. McKee, *Ann. Bot.* **67** (suppl.), 23 (1991).
2. J. M. Barnola, D. Raynaud, Y. S. Korotkevich, C. Lorius, *Nature* **329**, 408 (1987); A. Neftel, H. Oeschger, T. Staffelbach, E. Stauffer, *ibid.* **331**, 609 (1988); D. Raynaud *et al.*, *Science* **259**, 926 (1993); J. Jouzel *et al.*, *Nature* **364**, 407 (1993).
3. M. Leuenberger, U. Siegenthaler, C. C. Langway, *Nature* **357**, 488 (1992).
4. H. W. Polley, H. B. Johnson, B. D. Marino, H. S. Mayeux, *ibid.* **361**, 61 (1993).
5. J. L. Betancourt, T. R. Van Devender, P. S. Martin, Eds., *Packrat Middens: The Last 40,000 Years of Biotic Change* (Univ. of Arizona Press, Tucson, AZ, 1990).
6. F. I. Woodward and F. A. Bazzaz, *J. Exp. Bot.* **39**, 1771 (1988).
7. F. I. Woodward, *Nature* **327**, 617 (1987).
8. J. Peñuelas and R. Matamala, *J. Exp. Bot.* **41**, 1119 (1990); E. Paoletti and R. Gellini, *Acta Oecol.* **14**, 173 (1993); D. J. Beerling and W. G. Chaloner, *Ann. Bot.* **71**, 431 (1993).
9. J. Van Der Burgh, H. Visscher, D. L. Dilcher, W. M. Kürschner, *Science* **260**, 1788 (1993); see also D. J. Beerling and W. G. Chaloner, *Biol. J. Linn. Soc.* **48**, 343 (1993).
10. The C_3 plants use the Calvin cycle, which fixes CO_2 to ribulose-bisphosphate (RuBP) to form three-carbon products; RuBP also reacts with oxygen in photorespiration, releasing CO_2 into the atmosphere. In C_4 plants, including most tropical grasses and many halophytic shrubs, CO_2 reacts with phosphoenolpyruvate (PEP) to form four-carbon acids; PEP carboxylase has a low affinity for oxygen, so little CO_2 is lost in photorespiration. Increased levels of atmospheric CO_2 enhance the carbon fixation of C_3 plants by reducing energy loss by photorespiration. Values of $\delta^{13}C_{plant}$ for C_4 plants are much less dependent on C_i/C_a than those for C_3 plants; hence, $\delta^{13}C_{plant}$ of C_4 species would be influenced primarily by changes in $\delta^{13}C_{air}$ rather than by changing CO_2 levels. In contrast, $\delta^{13}C_{plant}$ of C_3 species should reveal more about physiological control of C_i/C_a in response to changing CO_2 levels superimposed on variations in $\delta^{13}C_{air}$.
11. G. D. Farquhar, M. H. O'Leary, J. A. Berry, *Aust. J. Plant Physiol.* **9**, 121 (1982).
12. Most work on stomatal densities of fossil leaves has involved broadleaf plants, for which analytical protocols have been established (*20*). In broadleaf plants, the ratio of the number of stomata per unit area to the number of stomata plus number of epidermal cells, or stomatal index, is measured to counter the effect of changing leaf area. Stomatal index cannot be measured conveniently in pine needles, where stomata run in recessed rows parallel to the long axis of the needle. Soaking in isopropyl alcohol for 30 to 40 min in a sonic cleaner removes the epicuticular wax plugs that usually occlude the stomata [F. Yoshie and A. Sakie, *Can. J. Bot.* **63**, 2150 (1985)]. After air-drying, samples were straightened and examined with a reflecting light microscope. Stomatal density was measured in the central portion of each needle, which tends to exhibit the least variability [W. Zelawski and T. Gowin, *Folia For. Pol. Ser. A* **13**, 111 (1967)]. At least 24 separate fields were measured along the middle third of each needle. Stomata were counted along each row for a prescribed distance defined from guard cell–florin ring intersection of the beginning stoma to a similar position further along the microscope's ocular scale. In regions with more than a single stomatal row, similar measurements were made on each row. After measurement of needle width, average density for each needle was calculated as number of stomata per square millimeter. Average stomatal density per midden was calculated from 22 to 33 needles in each sample. The relation between stomatal density and elevation is too inconsistent to warrant correction for elevation (*20*).
13. The terminal thirds of each of the needles were pooled for stable carbon isotope analysis. Each pooled sample was ground to 20-mesh (~ 1mm), and oils and resins were extracted with toluene-ethanol in a Soxhlet extraction apparatus. Holocellulose was isolated by treatment in an acidified sodium chlorite solution [J. W. Green, in *Methods of Carbohydrate Chemistry*, R. L. Whistler, Ed. (Academic Press, New York, 1963), p. 9; S. W. Leavitt and S. R. Danzer, *Anal. Chem.* **65**, 87 (1993)]. Holocellulose was combusted to CO_2 in a microcombustion system and cryogenically purified for mass-spectrometric analysis. The $\delta^{13}C$ results are reported in per mil units with respect to the Pee Dee belemnite (PDB) standard, and multiple combustions of a laboratory holocellulose standard during the project gave a standard deviation of 0.38 per mil. Despite this error, samples of different ages were run in a random sequence; there appears to be no systematic biasing of the results based on variability in the standards. The $\delta^{13}C$ values were normalized to modern sea level, on the basis of an average elevational gradient for forbs, shrubs, and trees of 1.2 mil^{-1} km^{-1} [Ch. Körner, G. D. Farquhar, Z. Roksandic, *Oecologia* **74**, 623 (1988); (*26*); P. V. Vitousek, C. B. Field, P. A. Matson, *ibid.* **84**, 362 (1990); A. D. Friend, F. I. Woodward, V. R. Switsur, *Funct. Ecol.* **3**, 117 (1989)]. To address the concern that our correction to sea level pushes isotope discrimination estimates upward, decreasing estimated $C_a - C_i$ while maintaining a constant difference between the estimates for each time period (that is, that we were calculating percent change on an artificially reduced base, exaggerating the magnitude of the effect), we corrected raw $\delta^{13}C$ values to the mean elevation of all of the sites (1824.5 m) and found that (i) the mean isotopic differences between periods remained virtually identical; (ii) absolute values of $C_a - C_i$ and WUE increased, but the glacial-Holocene differences increased from 13.6% and 14.6%, respectively, as originally calculated with sea-level corrected values, to 18.7% and 18.7% with the mean elevation corrected values; and (iii) absolute values of C_i went down, but the glacial-Holocene change increased from 62.0% calculated with sea-level corrected values to 66.2% with the mean corrected values. We also took uncorrected $\delta^{13}C$ values and calculated P_i and $P_a - P_i$ from C_a and $C_a - C_i$ using standard mean atmosphere tables. We found P_i and $P_a - P_i$ increased 51% and 19%, respectively, from glacial to Holocene, compared with our original sea-level corrected change of 62% and 14% for C_i and $C_a - C_i$, respectively. Thus, elevation-related effects do not change our general picture. We did not correct for latitudinal effects. The gradient of $\delta^{13}C_{plant}$ across 70° in latitude from Körner *et al.* (*26*) is based on a host of perennial herbaceous species from the coldest life zones from equatorial mountains to subpolar flats. If we apply their slope of −0.036 per mil per degree of latitude to our glacial sites versus the Holocene sites, which are on average 5° apart, then latitude would bias our limber pine series by −0.18 per mil. This would reduce our isotopic depletion from glacial to Holocene from an uncorrected −1.5 per mil to a corrected −1.3 per mil. We were uneasy about applying the latitudinal correction because the data of Körner *et al.* (*26*) may be contaminated by species or climatic effects. This is apparent in the nonlinearity of their slope, with relatively negative isotopic values reported for the subtropical zone. In any case, the latitudinal correction would not change our general conclusion that limber pine cellulose was isotopically depleted during the Holocene.
14. M. Stuiver and R. Kra, Eds., *Radiocarbon* **28**, 805–1030 (1986).
15. For U/Th corrections of ^{14}C ages, we used the linear regression of R. Zahn, T. F. Pedersen, B. D. Bornhold, and A. C. Mix [*Paleoceanography* **6**, 543 (1991)], which is based on data from Barbados corals developed by E. Bard, B. Hamelin, R. G. Fairbanks, and A. Zindler [*Nature* **345**, 405 (1990)].
16. J. R. Ehleringer, in *Carbon Isotope Techniques*, D. C. Coleman and B. Fry, Eds. (Academic Press, New York, 1991), pp. 187–200.
17. B. D. Marino, M. B. McElroy, R. J. Salawitch, W. G. Spaulding, *Nature* **357**, 461 (1992).
18. S. W. Wong, I. R. Cowan, G. D. Farquhar, *ibid.* **282**, 424 (1979); J. Masle, G. D. Farquhar, R. M. Gifford, *Aust. J. Plant Physiol.* **17**, 465 (1990).
19. G. D. Farquhar and T. D. Sharkey, *Annu. Rev. Plant Physiol.* **33**, 317 (1982).
20. D. J. Beerling and W. G. Chaloner, *Holocene* **2**, 71 (1992).
21. A. D. Friend and F. I. Woodward, *Adv. Ecol. Res.* **20**, 59 (1990).
22. W. M. Post *et al.*, *Am. Sci.* **78**, 31 (1990).
23. R. V. Krishnamurthy and S. Epstein, *Tellus Ser. B* **42**, 423 (1990); S. W. Leavitt and S. R. Danzer, *Nature* **352**, 671 (1991); *Radiocarbon* **34**, 783 (1992); T. B. Coplen, I. J. Winograd, J. M. Landwehr, A. C. Riggs, *Science* **263**, 361 (1994).
24. J. P. Jasper and J. M. Hayes, *Nature* **347**, 462 (1990); G. H. Rau, P. N. Froelich, T. Takahashi, D. J. Des Marais, *Paleoceanography* **6**, 335 (1991).
25. S. W. Leavitt and T. Newberry, *Plant Physiol. (Life Sci. Adv.)* **11**, 257 (1992).
26. Ch. Körner, G. D. Farquhar, S. C. Wong, *Oecologia* **88**, 30 (1991).
27. A. Neftel, E. Moor, H. Oeschger, B. Stauffer, *Nature* **315**, 45 (1985).
28. C. D. Keeling *et al.*, in *Aspects of Climate Variability in the Pacific and the Western Americas*, D.

H. Peterson, Ed., (AGU Mongr. 55, American Geophysical Union, Washington, DC, 1989), pp. 165–236.
29. C. J. Yapp and S. Epstein, *Earth Planet. Sci. Lett.* **34**, 333 (1977).
30. Altitude-normalized limber pine $\delta^{13}C$ values were averaged for each time period and 1.5 per mil was subtracted to account for observed holocellulose to whole-tissue isotopic differences [S. W. Leavitt and A. Long, *Nature* **298**, 742 (1982); *Chem. Geol.* **87**, 59 (1991)]. Discrimination (Δ) and C_i/C_a values were calculated with both sets of $\delta^{13}C_{air}$, and these results were averaged. Average atmospheric CO_2 concentrations were taken from (*3*).
31. We thank K. L. Cole, R. S. Thompson, W. G. Spaulding, P. E. Wigand, J. I. Mead, and L. Agenbroad for limber pine macrofossils; A. Neftel for CO_2 values from the Byrd ice core; M. Schiffer and D. Killick for access to their reflecting light microscope; D. Bentley for scanning electron microscopy images; A. J. T. Jull and D. Donahue for AMS dates; A. Long for discussion and technical support; S. Danzer and T. Newberry for sample preparation; and J. Ehleringer, R. Sage, H. B. Johnson, and I. Winograd for critical reading of the manuscript. Support provided by the state of Arizona and the U.S. Geological Survey's Global Change Program.

1 November 1993; accepted 7 February 1994

Quantifying Global Warming from the Retreat of Glaciers

Johannes Oerlemans

Records of glacier fluctuations compiled by the World Glacier Monitoring Service can be used to derive an independent estimate of global warming during the last 100 years. Records of different glaciers are made comparable by a two-step scaling procedure: one allowing for differences in glacier geometry, the other for differences in climate sensitivity. The retreat of glaciers during the last 100 years appears to be coherent over the globe. On the basis of modeling of the climate sensitivity of glaciers, the observed glacier retreat can be explained by a linear warming trend of 0.66 kelvin per century.

As suggested by many historic records, valley glaciers are sensitive indicators of climatic change (*1–5*). This large sensitivity is a consequence of the typical properties of a melting ice or snow surface. Because the surface temperature is fixed during melting, an increasing flow of energy to the surface, either by radiation or air motion, is used entirely for additional melting. In contrast, a normal surface would raise its temperature and radiate more energy upward to restore the balance.

The monitoring of glacier mass balance (annual mass gain or loss at the surface) is the best way to infer climatic change with glaciers. Although such measurements are being made on selected glaciers, the available records are short (<45 years, <30 years in most cases). Records of glacier length are much longer, some beginning around A.D. 1600, and can be used to provide information on climate variability. Many glaciers have retreated over the last 100 or 150 years (Fig. 1). Current understanding of glacier dynamics permits a quantification of the climate change needed to explain this retreat (in the same spirit as the use of tree-ring data or oxygen isotope values from ice cores). Although very discontinuous in time, the data points are reliable, especially with regard to the maximum glacier extent because the trimlines and moraine systems left behind can be studied. However, to provide information on global climate, the records must be scaled and considered together.

The climatic interpretation of a change in glacier length is hampered because response times are different for different glaciers (*5, 6*). For most valley glaciers, the response time is 10 to 50 years. When studies are in a significantly longer time scale, >75 years, a workable assumption is that the long-term change in glacier length largely reflects the dependence of the equilibrium glacier state on climate. More formally, climate and glacier fluctuations over a specific period can be viewed as composed of a linear trend on which smaller scale fluctuations are imposed. In this report, I try to find this linear component, thereby assuming that glacier extent is in balance with climate. This assumption will be more accurate when the period considered is longer. Here I consider the period 1850 to 1990 (but the average length of the records used is only 94 years).

In total, I used records from 48 glaciers in the analysis, considering data from only 1850 onward (Table 1) (*7–11*). I calculated linear trends of change in glacier length for all glaciers, irrespective of the start or end of the record. All glacier fronts appeared to have retreated; the mean rates were between 86 and 1.3 m/year. Next I used a two-step scaling procedure to make results from different glaciers comparable. The first step allows for the notion that glaciers with

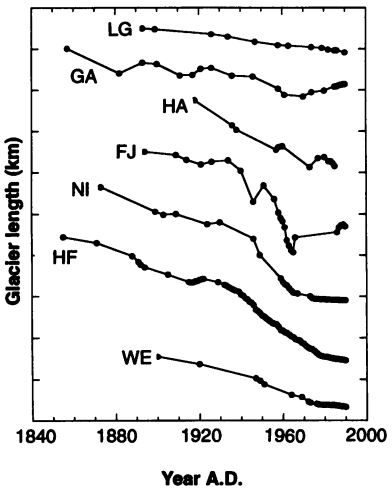

Fig. 1. Examples of fluctuations in glacier length. Data were compiled by the World Glacier Monitoring Service (Zürich), with some additions (*7*). Each dot represents an observation. Glaciers shown are Lewis Glacier (LG, Kenya), Glacier d'Argentière (GA, France), Hansbreen (HA, Spitsbergen), Franz Joseph Glacier (FJ, New Zealand), Nigardsbreen (NI, Norway), Hintereisferner (HF, Austria), and Wedgemount Glacier (WE, Canada). In these records, retreat has stopped or slowed as a response to the decrease in global temperature from 1950 to 1975 (*21, 22*). This observation suggests an effective glacier response time of about 25 years.

Table 1. Summary of the results for different regions. In total, data from 48 glaciers were used (*11*).

Region	Number of glaciers	Data source (reference)	Period	Mean trend (m/year)	Scaled mean trend (m/year)
Rocky Mountains	24	(*7*)	1890 to 1974	−15.2	−13.7
Spitsbergen	3	(*7*)	1906 to 1990	−51.7	−14.9
Iceland	1	(*8*)	1850 to 1965	−12.2	−6.3
Norway	2	(*7, 9*)	1850 to 1990	−28.7	−12.1
Alps	4	(*7*)	1850 to 1988	−15.6	−9.3
Central Asia	9	(*7*)	1874 to 1980	−9.9	−13.3
Irian Jaya	2	(*7*)	1936 to 1990	−25.9	−7.1
Kenya	2	(*7, 10*)	1893 to 1987	−4.8	−6.7
New Zealand	1	(*7*)	1894 to 1990	−25.9	−13.9

Institute for Marine and Atmospheric Research, Utrecht University, Princetonplein 5, 3584 CC Utrecht, Netherlands.